Journal of Sustainable Metallurgy
https://doi.org/10.1007/s40831-022-00612-x

THEMATIC SECTION: REWAS 2022: DEVELOPING TOMORROW'S TECHNICAL CYCLES

Thermal De-coating Pre-treatment for Loose or Compacted Aluminum Scrap and Consequences for Salt-Flux Recycling

Alicia Vallejo-Olivares[1] · Solveig Høgåsen[1] · Anne Kvithyld[2] · Gabriella Tranell[1]

Received: 9 June 2022 / Accepted: 6 October 2022

Abstract
In aluminum recycling, thermal de-coating pre-treatments remove moisture and organic contamination before re-melting. If the scrap is compacted into bales or briquettes before the thermal treatment and re-melting processes, less surface area is exposed to oxidation in contact with air. However, compaction may also limit the efficiency of the de-coating process. In this study, coated sheets of aluminum were thermally de-coated at varied temperatures and durations. Observations of changes in coating thickness, mass, color, and composition revealed a maximum de-coating efficiency of close to 75% wt due to remaining oxide residues. The relationship between de-coating and compaction was investigated by thermally treating loose shreddings (chips) and briquettes of various densities. The briquettes were compacted by three methods: uniaxial, moderate-pressure torsion (MPT), and MPT at 450 °C (Hot MPT); and the de-coating efficiency was calculated from the mass loss. Subsequently, the samples were re-melted under salt-flux and compared with another set of samples which were re-melted without thermal pre-treatment. The results showed that thermal de-coating significantly promotes the coalescence of loose chips and briquettes compacted uniaxially, up to similar coalescences than initially uncoated aluminum samples. Thermally treating the MPT briquettes, which were more densely compacted, led to less de-coating, and subsequently lower coalescences. The analysis of re-melted material revealed that the coating residues did not significantly affect the composition, while the compaction prevented Mg loss for the uncoated materials.

The contributing editor for this article was Zhi Sun.

✉ Alicia Vallejo-Olivares
alicia.v.olivares@ntnu.no

[1] Norwegian University of Science and Technology (NTNU), Trondheim, Norway

[2] SINTEF, Trondheim, Norway

Published online: 28 October 2022

Graphical Abstract

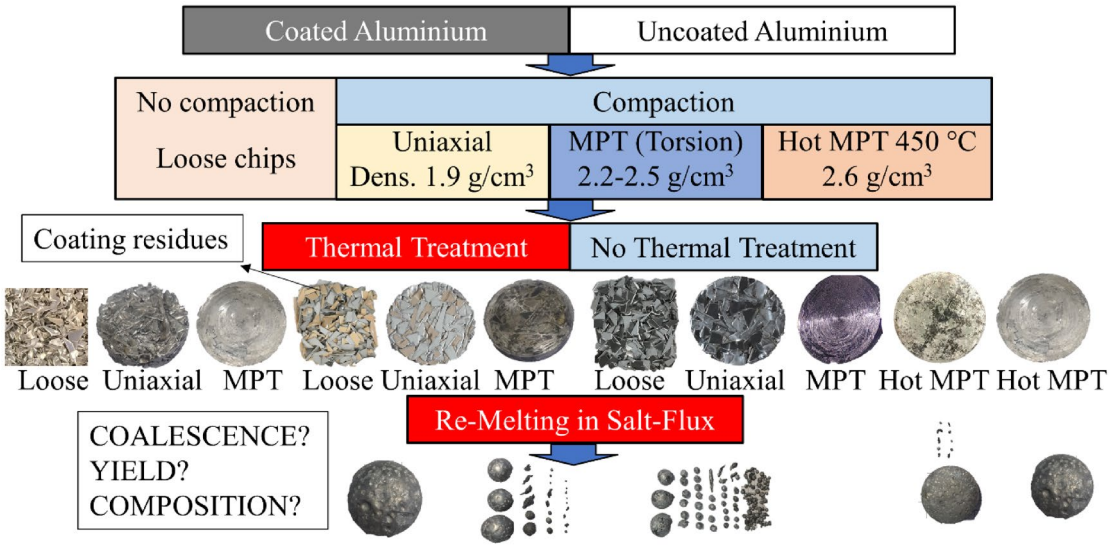

Keywords Recycling · Aluminum · Pre-treatment · Compaction · De-coating · Salt-flux

Introduction

In aluminum recycling, a thermal pre-treatment is often applied to post-consumer scrap in order to remove coatings, moisture, and other organics before re-melting [1]. Thermal pre-treatments are beneficial in many ways, such as lower dross generation, higher re-melting yield, and improved process control and melt cleanliness. Furthermore, re-melting contaminated scrap without treatment could lead to the formation of H_2S (g), PH_3 (g), H_2 (g), CH_4 (g) or dioxins, which are toxic, explosive or combustible [2]. An ideal thermal pre-treatment should remove the moisture and organic materials without oxidizing the metals while operating at the lowest possible cost and energy consumption. Regarding the process parameters, low temperatures may reduce metal oxidation and energy consumption but at the expense of an incomplete removal of the organics or longer times for completion. Kvithyld et al. [3] showed that the optimal parameters also depend on the chemical composition of the coating, the atmosphere (especially oxygen availability) and the heating rate.

Compacting the scrap into bales or briquettes is another standard recycling pre-treatment, since it facilitates storage and transport. A previous study [4] showed that compaction could reduce the oxidation of thin scrap, which has a high specific surface area. The correlation between scrap thickness and re-melting losses was previously described by Rossel [5]. However, the scrap bales are often broken down back into loose pieces before the sorting and thermal pre-treatments [6, 7]. Whether the scrap is loose or compacted during the thermal treatment may affect the removal of organics as it may alter scrap heat transfer and exposure to oxygen. Steglich [8] thermally treated bales of used beverage cans (UBCs) and foils and observed a correlation between the thermal conductivity of the bales and their density and porosity. According to Wells [9], the heat transferred through bales of UBCs is much lower than through a block of solid aluminum. In a later study, Steglich [10] re-melted UBC bales with different densities, organic content, and pre-treatment conditions. The results indicated that bales compacted more loosely formed less dross during re-melting, for a set-up consisting of a multi-chamber furnace with molten aluminum heel.

Another common method to re-melt post-consumer scrap is the use of rotary furnaces with salt-flux. The salt-flux, a mix of NaCl and KCl with small additions of fluorides, helps separating the molten metal from the oxides and contamination, promoting the coalescence of the metal droplets and preventing the melt from oxidation [1, 7]. The coalescence efficiency describes the ability of the individual aluminum pieces to merge into a macro phase. This is critical for a successful re-melting operation without too much metal loss trapped in the salt slag residues. Several studies have used the coalescence efficiency as an indicator for recyclability, and showed that it is influenced by furnace operation conditions [11, 12], the salt/scrap ratio [13], the concentration of fluorides [14], and non-metallic particles [15] in the salts and the surface area and contamination of the scrap [12, 16, 17]. Furthermore, the work of Capuzzi on small coated disks [14] and Gökelma

on coffee capsules [18] showed that thermal de-coating promoted the coalescence of coated scrap when re-melting under salt-flux, and in both cases, the results were better for the samples treated at higher temperatures (600 °C and 500 °C, respectively).

Another critical aspect of aluminum recycling is metal quality. Even if the thermal de-coating removes most organic and volatile elements from the scrap, some residues (e.g., oxides) remain and can act as a source of impurities or inclusions in the melt. For example, white inorganic pigments of TiO_2 are commonly found in aluminum packaging. Wang et al. [19], Li and Qui [20], and Önem [21] demonstrated the presence of these oxide residues on the the surface of UBCs after thermal de-coating. Wang also observed that the thermal de-coating removed up to 93% of the weight of the coating, in contrast to a 100% removal by chemical treatment. Whether the de-coating residues will accumulate in the melt or end up in the slag or salt-cake after re-melting was investigated by Meskers for magnesium alloys based on thermodynamic and kinetic mechanisms [22, 23] and by Rombach [24] for aluminum. Hiraki [25] evaluated the refining ability of salt-flux on aluminum secondary melts based on a thermodynamic model, and concluded that only Ho, Dy, Li, La, Mg, Gd, Ce, Yb, Ca, and Sr could be removed from the melt by reaction with chloride salts. Oosumi [26] studied the accumulation of Ti experimentally by re-melting (without salt-flux) UBCs after thermal or chemical de-coating treatments, observing higher Ti concentrations for the recycled aluminum that had been thermally de-coated than the chemically de-coated. The concern over the accumulation of impurities and alloying elements in aluminum recycling is associated with the lack of successful refining methods. Løvik et al. [27] argued that the impurity accumulation would be a challenge even with closed-loop recycling systems such as that of UBCs. Several researchers, such as Castro [28] and Reuter [29], have emphasized the criticality of optimizing scrap collection and sorting techniques, as well as proposing a design-for-recycling approach in an attempt to overcome these metallurgical challenges for the circular economy.

To contribute to the state of the art, this study evaluates the de-coating efficiency of coated aluminum sheets at various temperatures and durations by measuring the changes in weight and coating thickness, and the composition of the de-coating residues. The relationship between the compaction state of the scrap and the de-coating efficiency and re-melting losses in salt-flux is further investigated, comparing coated and uncoated sheets of clean, as-produced aluminum. Finally, the recycled metal is analyzed to determine whether the application of thermal de-coating or compaction routes influences its chemical composition.

Materials and Method

This study is divided into two parts. The first aims to find the optimal thermal de-coating parameters for the coated sheet by testing a range of temperatures and durations, and the second part investigates the effects of combining mechanical and thermal pre-treatments before re-melting under salt-flux. The materials were two coils of aluminum sheet alloy AA8111 of 600 µm thickness, one coated and the other uncoated. The main alloying elements for both sheets are displayed in Table 1, and the detailed composition including trace elements in Table 4, where it is also compared to the compositions of the samples after re-melting.

Thermal De-coating Optimization: Time and Temperature Variations

For the optimisation study, the coated sheet was cut into rectangles of an area of 10 × 5 cm, weighing 8–9 g. A subset of these samples was thermally treated at a constant temperature of 550 °C and durations of 5, 10, 20, 30, 40, 50, and 60 min, and the second subset at temperatures 450 °C, 550 °C, and 600 °C for 5 and 10 min. The samples were introduced into a pre-heated Nabertherm muffle furnace with exhaust and were taken out to cool down at room temperature after the treatment. The efficiency of the de-coating treatment was assessed based on several observations: changes in mass, coating thickness, elemental composition, and the visual appearance, particularly the color when comparing the samples before and after the treatment. Part of the coating remained adhered to the aluminum after the thermal treatment. For one of the sheets, all coating rests were removed by washing with ethanol. The dry and clean sheet weighed 0.22 g less than before the thermal treatment. This value was accepted as the standard coating mass for the sheet samples, and the de-coating efficiencies were calculated as the percentage ratio of the mass loss to the standard coating mass. Calculating the de-coating efficiencies makes it possible to compare with other de-coating methods used in literature, such as acid leaching in Wang et al. [19]

Table 1 Compositions of the aluminum sheets analyzed by ICP-MS

	Al (%)	Fe (%)	Si (%)	Mg (ppm)	Cu (ppm)	Ga (ppm)	V (ppm)	Ti (ppm)	Mn (ppm)	Zn (ppm)
Coated	96.87	0.75	0.23	7	11	114	84	99	27	23
Uncoated	98.10	0.81	0.23	404	340	106	208	53	377	75

Combination of Compaction and Thermal Pre-treatments

Both coated and uncoated aluminum were used to study the influence of compaction in the thermal pre-treatment. The sample preparation began by shredding the sheets into chips and sieving them to unify their size. Next, some chips were compacted by one of the three routes described below, and some were left uncompacted (referred to as "loose chips"). Half of the samples were then thermally treated, and finally, all the samples were re-melted under salt-flux. The experimental procedure is shown schematically in the graphical abstract.

Shredding

The shredding machine was a Getecha RS 1600-A1.1.1 with a grate of 8 mm diameter. The shredded chips were sieved with two square mesh sieves of 2–5 mm^2. Image analysis of 700 sieved fragments with the software ImageJ revealed an average area of 0.26 cm^2 and median area of 0.24 cm^2 for the uncoated chips and 0.26 cm^2 average and 0.23 cm^2 median for the coated chips, with a standard deviation of 0.14 cm^2 for both materials. The average weight per chip was estimated by dividing the weight of the chips analyzed by their number. The mean weight was 49.0 mg for the uncoated and 48.4 mg for the coated chips.

Compaction

The chips were compressed into cylindrical briquettes of 4 cm diameter, each weighing 20 g, using a hydraulic press MTS 311. One subset was compacted by holding a 100 kN (80 MPa) uniaxial force during 5 s. This method is referred to as "uniaxial." Another sub-group was compacted by moderate-pressure torsion (MPT), where the piston applied a uniaxial force of 70 kN (56 MPa), while the mold rotated 360° four times for 200 s. Finally, a third subset was compacted by MPT under 450 °C (Hot MPT).

One briquette sample from each sub-group was analyzed by computed tomography (CT), giving a set of slices used to measure the internal porosity. The analysis was performed using the software ImageJ; this procedure was described in a previous study [30]. Table 2 presents the average bulk densities and the briquette internal porosities. The porosity presented for each sample is the average of between 80 and 250 images, and the standard deviation within a sample is also displayed. Slices close to the top and bottom of the briquette were omitted.

The bulk densities of the coated chips were lower than for the uncoated. In most cases, some loose chips fell off when taking them out of the mold and in further handling, especially for the briquettes compacted by the uniaxial method. The internal porosity was significantly lower when compacting by the MPT method and essentially non-existent by Hot MPT.

Thermal De-coating

No treatment was applied to the Hot MPT briquettes since the method, reaching temperatures of 450 °C, would simultaneously serve as thermal treatment and compaction. Out of the rest of the samples, half were treated by the procedure described above but with constant parameters of 1 h and 550 °C and half were left untreated.

Re-melting

The re-melting was carried out in a Nabertherm resistance furnace. Three ceramic crucibles (Al_2O_3–SiO_2) of 20 cl volume, filled with 80 g of mixed salts with composition ratios (%wt) of 68.6:29.4:2.0 NaCl:KCl:CaF_2 were placed in the furnace at 800 °C. The amount of salt-flux used relative to the non-metallic content of the scrap is significantly higher than those typically used in industrial rotary furnaces, as reported by Capuzzi [13]. For the present static set-up, a salt/scrap ratio of 4 was required so that the chips would be completely covered by the molten salts and protected from oxidation. The aluminum samples, either briquettes or batches of loose chips weighing 20 g each, were added to the crucibles once the salt was molten (after approx. 40 min). The crucibles were then held in the closed furnace for 10 min at 800 °C, removed, and cooled in air. Stirring was not applied. For the chips and briquettes of coated material that had not been thermally pre-treated, the spontaneous combustion of the coating generated flames and dark smoke for around 30 s. The furnace was kept open until the end of this combustion. Once the crucibles were at room temperature, the salt was separated from the metal by crushing and washing it with water on an 0.8 mm sieve. After drying, the metal pieces were weighed, and the metal yield and coalescence were calculated using Eqs. 1 and 2.

Table 2 Average briquette bulk density (g/cm^3) and internal porosity (%) for the different compaction routes

	Uniaxial		MPT		Hot MPT	
	Porosity	Density	Porosity	Density	Porosity	Density
Uncoated	16.64 ± 1.37	1.94 ± 0.01	0.68 ± 0.84	2.46 ± 0.01	0.04 ± 0.04	2.60 ± 0.02
Coated	14.70 ± 1.43	1.90 ± 0.18	4.48 ± 1.65	2.19 ± 0.09	0.06 ± 0.11	2.54 ± 0.07

$$\%\text{Metal Yield} = \frac{m_{\text{recov}}}{m_{\text{input}}} * 100, \quad (1)$$

$$\%\text{Coalesced} = \frac{m_{\text{coalesced}}}{m_{\text{input}}} * 100, \quad (2)$$

where m_{recov} is the sum of the masses of the pieces recovered, m_{input} is the mass of the briquette or batch of chips before re-melting, and $m_{\text{coalesced}}$ is the mass of the largest piece recovered (shown in Fig. 6a).

Characterization Methods

The composition and thickness of the coating were studied by scanning electron microscopy (SEM) and optical microscopy (OM). On one side of the sheet, the coating was thinner (5 µm) and light in appearance, while on the other side, the coating was five times thicker (25 µm) and dark gray. The cross-sections of the dark coating were analyzed by SEM–EDS point analysis (Zeiss Ultra 55LE FEG-SEM) and by Electron Probe Micro Analysis (EPMA), for several samples before and after the thermal treatment. This way, it was possible to study the influence of the treatment time and temperature in the removal of specific elements. The de-coating residues formed a white/yellowish powder, which was analyzed by X-Ray Diffraction (XRD) in a DaVinci 1 X-ray Diffractometer using angles between 15° and 80° and a scan time of 30 min, and the qualitative phase identification was carried out with the software DIFFRAC.EVA. Finally, slices weighing approximately 1 g were cut from the re-melted metals and from the original sheets and sent for ICP-MS elemental analysis to ALS Scandinavia. The coated sheet was thermally treated at 550 °C for 1 h and cleaned with ethanol to remove the coating, and all samples were pre-digested with HCl and HNO_3.

Results and Discussion

Thermal De-coating Optimisation: Time and Temperature Variations

The results showed that heating duration and temperature affect the weight change, the coating thickness, and composition. Figure 1 shows an untreated sample, placed in the far left, next to samples treated at 550 °C with increasing treatment durations to the right.

A color change occurred for the coatings on both sides of the samples. For the samples thermally treated for 5 and 10 min, the color became darker than the original color. For treatments of 20 min and longer the differences were minor, therefore sheets treated at 30, 40, 50 and 60 min are not shown in Fig. 1. Similar color changes were also described by Kvithyld [3], who attributed the darker color to char residues from the decomposition of the coating by scission and the white color as a sign of a complete combustion of the carbon residues. When handling the samples, it was also observed that longer times resulted in the coating more easily flaking off. Note that the sheets were stored in sample bags before the pictures were taken; therefore, the flaking seems more intense than it was right after the treatment. Figure 2a presents the weight losses during de-coating after the treatments at 550 °C, and Fig. 2b for the 5- and 10-min treatments at varied temperatures. The bar graphs show the mean weight loss as a percentage of the sheets' initial weight and the variations within the three repetitions.

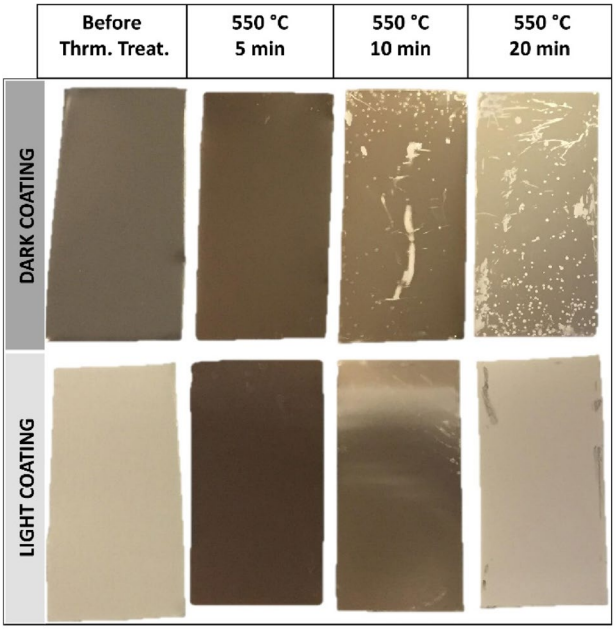

Fig. 1 Variations in dark side coating (above) and light side coating color (below) after thermal treatment

For the experimental series at 550 °C (Fig. 2a), the weight reduction increased with the treatment time up to 20 min, while after this point, the difference stagnated. The subset thermally treated for 20 min experienced the most significant weight decrease: − 1.8% wt. This was 74.5% of the total weight of the coating, meaning that this coating has a higher ratio of inorganic components than the UBCs studied by Wang [19]. Since the weight change did not increase for longer durations than 20 min, this seems to be the optimal treatment duration for the sheets. This is supported by the visual inspection of the samples in Fig. 1; the color differences after 20 min were minor. The results suggest that around 25% wt of this coating is not removable by thermal treatment. The treatments at 5 and 10 min removed 66.7% and 70.7% wt of the coating (corresponding to sheet's weight

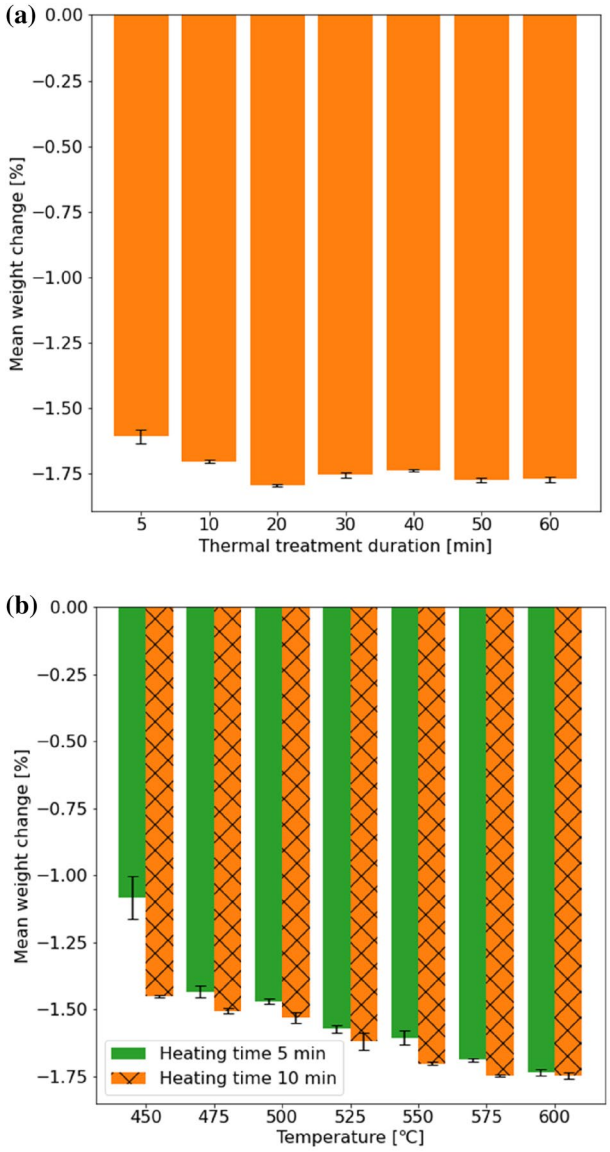

Fig. 2 Left: **a** Weight change due to thermal treatment at 550 °C and durations between 5 and 60 min. Right: **b** Weight change due to thermal treatment for 5 and 10 min at temperatures from 450 to 600 °C. Three repetitions each trial

changes − 1.6% and − 1.7% wt), which indicated that the thermal treatment was still incomplete. Figure 2b shows the result for the second subset of experiments that explored the possibilities of achieving complete de-coatings at 5 or 10 min by varying the temperature. The results show larger weight changes as temperatures increase. The largest de-coating efficiency was obtained at 600 °C and 10 min: 72.1%, corresponding to a weight loss of -1.8%. However, this is still slightly lower than for the samples treated 20 min at 550 °C in the first series of experiments. The sheets treated for 5 min at 450 °C led to the lowest de-coatings efficiency: 45.0% (− 1.1% wt decrease). Another trend was

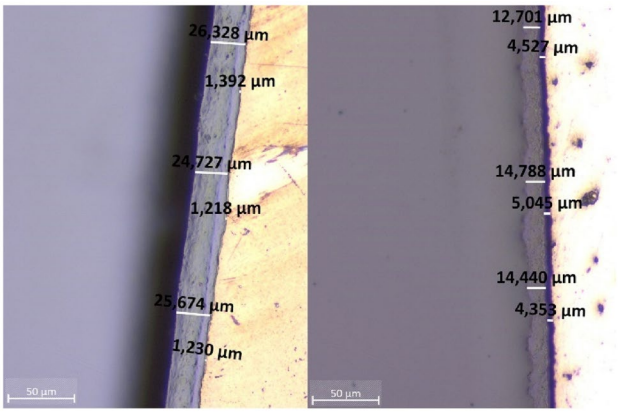

Fig. 3 Coating and void thickness measured by OM for an untreated sample (left) and a sample treated at 550 °C for 60 min (right)

that the difference in weight change between 5- and 10-min treatment times was more pronounced at lower temperatures. Figure 3 shows optical microscope images used to measure the thickness of the dark coating before and after thermal treatment. The images confirmed the partial removal of the coating after thermal treatment, as the coating is thinner in the treated samples than in the non-treated (untreated) sample. This analysis, performed on the samples treated at 550 °C, showed no significant differences between the treatment durations. The thickness decreased, on average, from an initial 25 µm before thermal treatment to 14 µm. This average was calculated out of 21 measurements, 3 in each sample. Treatments of 5, 10, 20, 30, 40, and 50 min are not shown in Fig. 3 but were included in the averages. It was also possible to observe a void between the aluminum surface and the coating, measuring on average 4 µm for the treated samples.

In both SEM (displayed in [30]) and EPMA images, it was observed that the coating was composed of a polymeric matrix and oxide filler particles. An SEM–EDS point analysis taken in one of the particles revealed a composition of 21.3% wt O, 20.8% wt Ca, 12.3% wt Ti, 4.8% wt Si, and 23.8% wt C. The carbon composition is uncertain in this analysis, but the findings suggest the presence of pigments or filler particles such as TiO_2, CaO, and SiO_2. In addition, the EPMA analysis of the coating before thermal treatment, displayed in Fig. 4, revealed that the coating is composed of higher concentrations of the elements carbon, silicon, oxygen, titanium, barium, and sulfur. The EPMA images are a semi-quantitative color mapping where brighter white, green, and red colors represent a higher concentration than black and blue.

These concentrations did not change after the thermal treatment, except for oxygen and carbon, shown in Fig. 5.

Changes in oxygen and carbon concentrations can be observed already after a 5-min treatment. This is likely

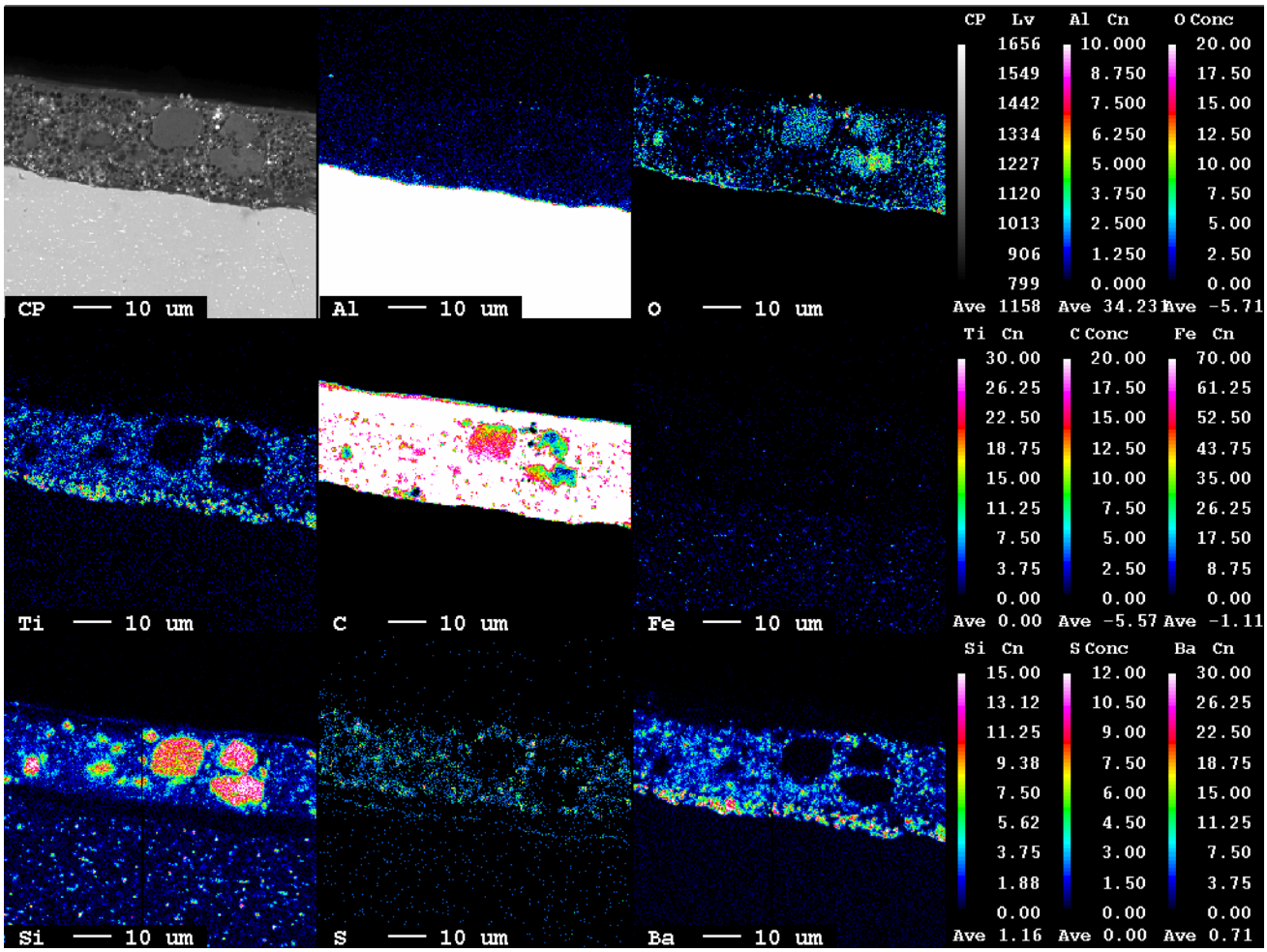

Fig. 4 EPMA analysis of the cross-section of the coated aluminum sheet. The color scale is in % (Color figure online)

related to the release of hydrocarbons or the formation of combustion gas products such as CO or CO_2. Still, after treatments of 60 min, high concentrations of C and O remain, possibly as oxide and carbide residues. Note that the carbon-containing epoxy resin used for sample preparation can affect the results.

An XRD analysis of the powder residue scraped off the samples treated for 5, 10, and 60 min at 550 °C identified the three main phases as $BaSO_4$, TiO_2, and SiO_2. The three analysis gave similar results, and one of the XRD patterns can be found in the supplementary material. $BaSO_4$ and TiO_2 have been previously highlighted as common components in organic coatings of magnesium alloys [31], as well as SiO_2, CaO, and Cr_2O_3 which are sometimes found in both organic and conversion/anodizing coatings. In a recent study, Önen et al. [21] characterized the coatings of several aluminum packaging products (UBCs, coffee capsules, and cosmetic cream tubes) and their thermal de-coating behavior. They observed that for those scraps, containing inner and outer coatings of thicknesses between 5 and 20 µm, a treatment of 500 °C and 15 min was sufficient to remove most of the organics leaving an apparently clean outer surface. However, even if the surface appeared clean after thermal treatment, the study also identified the presence of carbon and titanium residues by XRD analysis. One of the applications of the sheets in the current study is roofing plates, and the coating composition may thus differ from the typical coatings applied to packaging products and subsequently display different residues after thermal treatment.

Combination of Compaction and Thermal Pre-treatments

Thermal De-coating

The uniaxially compacted briquettes lost, on average, the same weight as the loose chips: 1.7% wt, and the weight loss for the MPT briquettes was smaller: 1.5% (out of initial weights of 20 g). Therefore, the results suggest that the uniaxial compaction did not affect the thermal de-coating, while

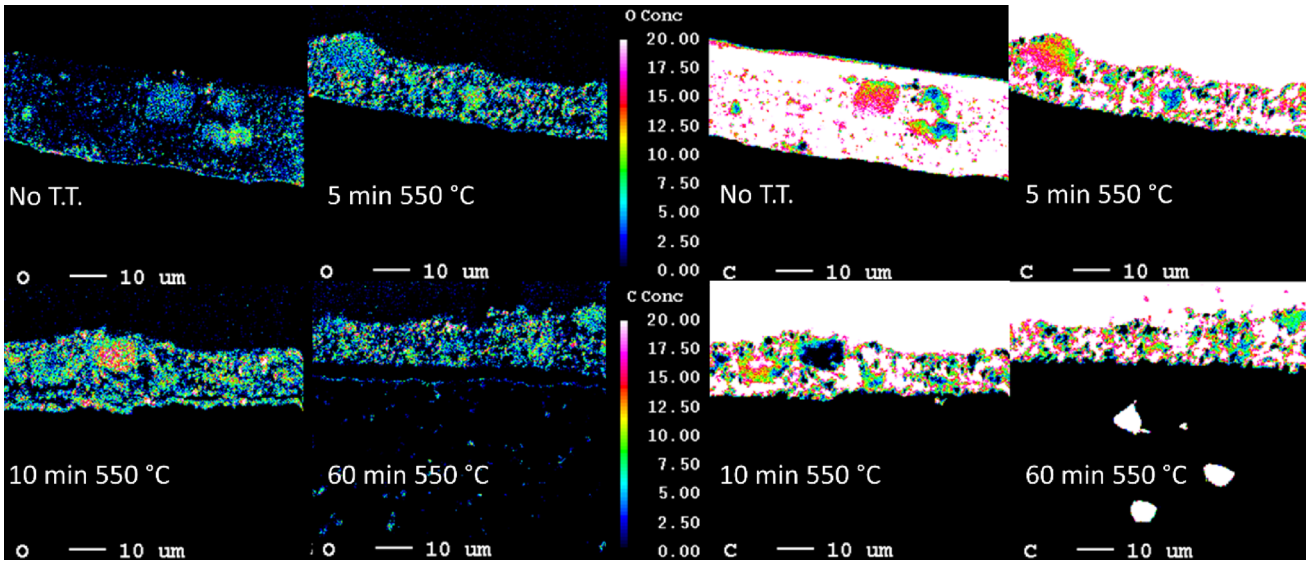

Fig. 5 Change in oxygen (left) and carbon (right) concentration from EPMA analysis. The color scale is in % (Color figure online)

MPT compaction slightly reduced the de-coating efficiency. The fact that the uniaxial compaction, even up to densities of 2 g/cm^3, does not affect the heat-treatment compared to the loose chips opposes some of Steglich's [10] observations, where bales compacted uniaxially to higher densities (1.11 g/cm^3) generated higher dross than those compacted to lower densities (0.69 g/cm^3) which was explained by an incomplete de-coating. Crucial differences in re-melting method (submersion in aluminum melt without salt-flux) and material (UBC post-consumer scrap) may cause the deviating observations. The weight change of the uncoated samples during treatment was also measured in a previous study [30]. All uncoated samples experienced a weight increase lower than 0.02%, which is attributed to oxidation and considered negligible compared to the de-coating weight loss in the coated samples.

Re-melting Coalescence

The material recovered after re-melting showed various degrees of coalescence. Good coalescence leads to most of the re-melted material merging into one round piece. On the contrary, poor coalescence leads to multiple tiny pearls distributed in the salt. A coalescence analysis can be done by comparing the images in Fig. 6a or the average coalescences for the different routes in Fig. 6b. All coalescence results are displayed in Table 3, in the following sub-section, together with the metal yield values.

The surfaces of the metal recovered from the coated, untreated samples appear rougher and darker because of the spontaneous combustion during their re-melting. On the contrary, the re-melted uncoated, and de-coated materials look smooth and shiny. The results prove, in agreement with literature [14, 18], that applying a thermal de-coating pre-treatment greatly improves the coalescence of the coated materials. Regarding the compaction route, thermally de-coating either loose chips or uniaxial briquettes resulted in similar coalescences to those of the uncoated materials. However, the coalescence was lower for the de-coated MPT briquettes. The reason may be that the MPT briquettes are so tightly compacted that oxygen cannot penetrate into the briquette, partly inhibiting the de-coating, as previously suggested by Steglich [32], and consequently, the resulting residues limit the ability of chips to coalesce together as also suggested by Capuzzi [14]. These results are consistent with the previous section. The uncoated material reached almost perfect coalescences regardless of the pre-treatment routes and a slight increase can be observed for the MPT and Hot MPT samples.

Re-melting Metal Yield

Table 3 contains the coalescence and metal yield results for all re-melting experiments. For comparisons between samples with significantly different non-metallic contents, comparing the metal recovery values may be more representative. For the present materials, however, the organic content was less than 2%, and therefore, the difference between metal recovery and metal yield would be approximately 1–2%, as calculated in [30].

The metal yield differences between pre-treatment routes are very small. If only the metal yields were evaluated, all the re-melting results would lie within 94–100%. These results would not explain the apparent differences observed

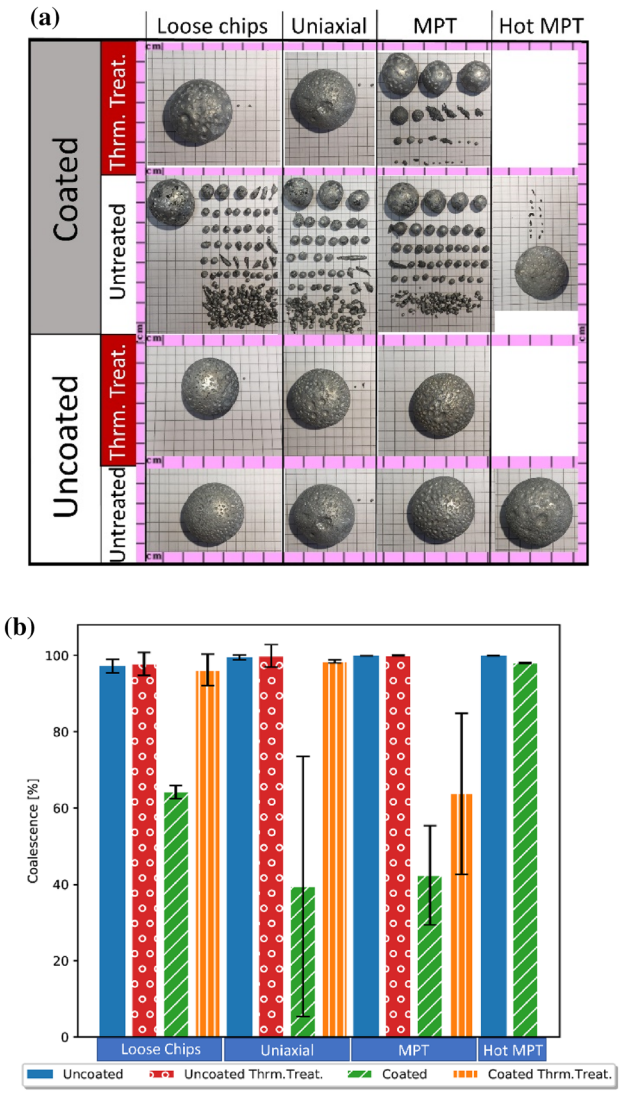

Fig. 6 Left: **a** Example of the recovered metal for each compaction and thermal pre-treatment routes. Right: **b** Average coalescence results for all re-melting experiments. The bars show the standard deviation (2 repetitions for Hot MPT, 3 for the rest)

on the re-melting products obtained via the different pre-treatment routes (Fig. 6a). In contrast, the coalescence variations can become as high as 90% when comparing coated thermally treated or coated untreated samples.

Composition of Recycled Metal

The ICP-MS analysis aimed to evaluate whether the choice of different compaction or thermal pre-treatment routes would affect the composition of the recovered aluminum. Table 4 contains the average results for both coated and uncoated material, and the number of repetitions per sample type is also indicated. For the coated re-melted samples, two had been thermally pre-treated before re-melting and two had not. Out of the three re-melted uncoated samples analyzed, two had been thermally treated, and one had not. Since it was not possible to observe any trend related to the application of the thermal pre-treatment or not, samples were classified by their compaction state. Some concentrations were lower than their detection limits for this analysis, so Li (< 5 ppm), Ca (< 200 ppm), Ba (< 10 ppm), In (< 0.1 ppm, Hg (< 0.04 ppm), Be (< 0.02 ppm) ,and Cd (< 0.03 ppm) are not displayed. For the coated aluminum, this was also the case for the Mg results in 5 samples (< 20 ppm) for two uniaxial briquettes, two MPT briquettes, and the one Hot MPT briquette. Thus, the results of Mg come from only two repetitions for both the uniaxial and MPT briquettes in the coated Al.

For the coated materials, there was a minor increase of some alloying elements after re-melting (Fe, Mn, Cu, Cr, and Mg), which is lower for the more compacted samples than for the loose samples. However, the standard deviations are larger than the differences between sample types and hence no firm conclusion may be drawn as to whether the inorganic coating residues contaminate the aluminum melt during re-melting with salt-flux. The Ti accumulation

Table 3 Coalescence (C) and metal yield (Y) results

Compaction	Loose chips				Uniaxial				MPT				Hot MPT	
Therm. Tr	No		Yes		No		Yes		No		Yes		No	
result	C	Y	C	Y	C	Y	C	Y	C	Y	C	Y	C	Y
Uncoated	95	95	94	94	100	100	103	103	100	100	100	100	100	100
Uncoated	98	98	100	100	100	100	100	100	100	100	100	100	100	100
Uncoated	99	99	100	100	99	99	96	96	100	100	100	100	–	
Average	97	97	98	98	99	100	100	100	100	100	100	100	100	
Std. dev	1.7	1.6	3.0	3.0	0.6	0.6	3.0	3.0	0.0	0.0	0.1	0.1	0.0	
Coated	65	96	90	100	85	95	98	98	29	96	62	97	98	98
Coated	62	94	99	99	3	96	99	99	60	96	91	95	98	98
Coated	66	97	99	99	30	94	99	99	39	96	39	96	–	
Average	64	96	96	99	40	95	98	98	42	96	64	96	98	
Std. dev	1.8	1.3	4.0	0.4	34.0	1.1	0.4	0.4	13.0	0.1	21.0	0.6	0.1	

Table 4 Averages and standard deviation of the 29 composition analyses by ICP-MS

	Coated aluminum					Uncoated aluminum				
Re-melted	No	Yes				No	Yes			
Sample	Sheet	Loose chips	Uniaxial briquettes	MPT briquettes	Hot MPT briquette	Sheet	Loose chips	Uniaxial briquettes	MPT briquettes	Hot MPT briquette
Nr. rep	3	4	4	4	1	3	3	3	3	1
Al (wt%)	96.87 ± 0.94	99.10 ± 0.80	99.13 ± 0.71	97.02 ± 0.65	96.00	98.10 ± 1.56	98.43 ± 0.95	98.1 ± 2.33	98.10 ± 0.83	99.50
Fe (%)	0.75 ± 0.01	0.80 ± 0.05	0.78 ± 0.03	0.76 ± 0.02	0.76	0.81 ± 0.01	0.83 ± 0.01	0.82 ± 0.03	0.83 ± 0.01	0.85
Si (%)	0.23 ± 0.03	0.23 ± 0.02	0.21 ± 0.02	0.21 ± 0.02	0.21	0.23 ± 0.02	0.16 ± 0.00	0.15 ± 0.01	0.15 ± 0.01	0.15
B (ppm)	7.30 ± 0.23	8.58 ± 4.80	6.81 ± 1.06	5.55 ± 0.75	2.35	4.78 ± 0.13	4.47 ± 0.41	4.19 ± 0.14	3.69 ± 0.29	3.41
Cd (ppm)	0.02 ± 0.00	0.10 ± 0.07	0.17 ± 0.08	0.10 ± 0.06	< 0.03	0.10 ± 0.01	0.15 ± 0.01	0.27 ± 0.11	0.19 ± 0.10	0.123
Co (ppm)	1.82 ± 0.04	1.92 ± 0.10	1.91 ± 0.07	1.77 ± 0.04	1.76	2.86 ± 0.07	2.83 ± 0.07	2.74 ± 0.06	2.84 ± 0.11	2.78
Cr (ppm)	7.78 ± 0.17	17.93 ± 3.19	15.58 ± 3.45	14.85 ± 4.24	8.56	15.60 ± 0.16	19.33 ± 4.67	17.73 ± 2.47	18.27 ± 0.87	19
Cu (ppm)	10.93 ± 0.40	32.43 ± 8.29	25.80 ± 4.27	22.50 ± 6.67	14.5	340.00 ± 6.38	348.00 ± 12.75	339.33 ± 4.11	354.67 ± 16.21	372
Ga (ppm)	114.00 ± 1.41	113.00 ± 6.04	111.75 ± 5.31	109.00 ± 6.75	103	106.33 ± 1.70	106.07 ± 6.09	103.30 ± 5.95	106.67 ± 4.03	98.8
Mg (ppm)	6.90 ± 0.16	16.09 ± 6.90	15.05 ± 3.55	13.15 ± 1.35	< 20	404.00 ± 5.35	131.00 ± 27.80	234.33 ± 48.61	267.00 ± 28.33	251
Mn (ppm)	26.63 ± 0.49	34.78 ± 2.40	32.25 ± 1.44	30.45 ± 2.21	29.2	366.00 ± 6.16	376.67 ± 3.09	367.00 ± 1.63	370.00 ± 1.41	383
Ni (ppm)	39.80 ± 0.22	42.50 ± 3.53	40.68 ± 1.99	38.53 ± 1.23	39.9	30.20 ± 0.94	31.93 ± 1.31	30.77 ± 0.66	31.40 ± 2.08	32.3
P (ppm)	3.64 ± 0.41	2.01 ± 0.20	3.15 ± 1.47	3.00 ± 0.59	2.54	1.93 ± 0.11	1.66 ± 0.22	2.93 ± 1.42	2.35 ± 0.86	2.19
Pb (ppm)	9.53 ± 0.13	10.59 ± 1.05	9.67 ± 0.33	9.29 ± 0.27	9.99	14.43 ± 0.12	14.87 ± 0.47	15.03 ± 0.05	15.03 ± 0.58	15.4
Sn (ppm)	1.93 ± 0.01	2.59 ± 0.74	2.04 ± 0.06	1.94 ± 0.07	1.94	2.45 ± 0.50	8.90 ± 7.92	3.35 ± 0.14	3.24 ± 0.11	3.44
Sr (ppm)	0.15 ± 0.01	0.59 ± 0.71	0.36 ± 0.21	0.16 ± 0.05	0.16	0.28 ± 0.08	0.74 ± 0.00	0.21 ± 0.13	0.10 ± 0.02	0.211
Ti (ppm)	99.37 ± 1.16	102.48 ± 4.54	101.10 ± 7.75	99.65 ± 1.93	105	53.03 ± 1.62	57.53 ± 3.74	56.70 ± 2.27	53.33 ± 0.69	56.5
V (ppm)	83.77 ± 1.87	82.90 ± 7.27	82.83 ± 4.94	84.70 ± 1.86	86	207.67 ± 0.94	212.00 ± 2.16	219.33 ± 4.19	213.00 ± 2.16	211
Zn (ppm)	22.50 ± 1.84	24.58 ± 1.41	25.60 ± 2.41	24.28 ± 2.05	23.5	74.40 ± 2.48	79.60 ± 2.84	79.43 ± 1.76	77.53 ± 3.90	80.6
Zr (ppm)	15.83 ± 0.40	17.88 ± 1.43	18.13 ± 1.75	18.35 ± 2.09	20.6	6.82 ± 0.27	7.33 ± 0.55	7.56 ± 0.76	7.65 ± 0.83	8.77

observed by Oosumi in UBC re-meltings without salt-flux [26] could not be replicated.

For the uncoated material, Fig. 7 shows the normalized concentration differences, calculated by subtracting the average concentration of each re-melted sample group from the average of the original sheets, and dividing it by the concentration of the original sheets. Decreases in specific elements after re-melting could indicate their removal from the melt due to reaction with the molten salt-flux.

If the initial concentrations were very low, increases of just a few ppm would stand out in the normalized comparison. Therefore, elements of concentrations lower than 10 ppm were not included in the graph. Figure 7 shows that Mg decreases during re-melting of the uncoated samples and that the Mg loss can be reduced by compacting the material. Figure 7 also shows a consistent decrease in the Si concentration after re-melting, regardless of the compaction. As for the rest of the results, the slight increases observed cannot be explained by the contamination from the coating since these samples were not coated. Furthermore, by looking again at Table 4, the standard deviations between the samples are of the same magnitude as the difference between samples.

In conclusion, the most significant result is that compaction leads to lower Mg reduction. This is supported by Hiraki's [25] thermodynamic analysis, showing the tendency of Mg to be refined from aluminum secondary melts by reaction with the salt-flux. The results suggest that by compacting the loose chips, the surface area exposed to the salt-flux is reduced, and as a result, Mg loss is partially prevented. The influence of compaction in the removal of Mg during salt-flux re-melting was also observed in [33]. Mg loss is a challenge during industrial re-melting operations, and the effect of compacting clean, Mg containing scrap, or even the Mg chips added during re-melting operations should be explored at a larger scale.

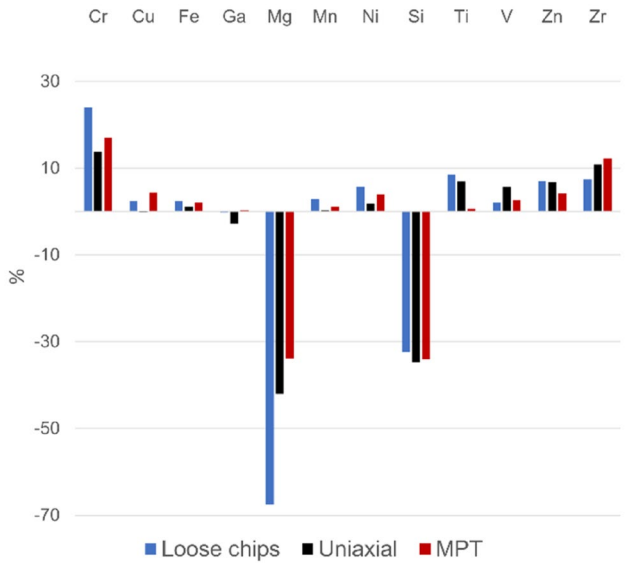

Fig. 7 Normalized concentration changes for the uncoated samples

Conclusions

The current work has investigated the interaction between the compaction and thermal de-coating pre-treatments for coated and uncoated aluminum. The performance of thermal de-coating and re-melting in salt-flux was assessed in terms of recycling metal yield, coalescence, and composition, leading to the following conclusions:

- Observations of changes in coating thickness, mass, color, and composition revealed a maximum de-coating efficiency of close to 75% wt, achieved after 20 min of treatment at 550 °C.
- The thermal de-coating was not affected by compacting the briquettes uniaxially (1.9 g/cm^3 density), but MPT compaction (2.2 g/cm^3 density) decreased the de-coating efficiency.
- The coalescence of the coated samples significantly improved due to the thermal de-coating similarly for the loose chips and uniaxially compacted briquettes (over 95%), but to a lower extent for the MPT compacted briquettes (64%).
- All metals yield results ranged between 94 and 100% for the different pre-treatment routes.
- Oxide residues (Ti, Si, S, Ba) remained attached to the material after thermal de-coating but were not associated with an increase in impurity concentration in the re-melted metal.
- Compaction may reduce Mg losses during salt-flux re-melting.

Supplementary Information The online version contains supplementary material available at https://doi.org/10.1007/s40831-022-00612-x.

Acknowledgements The authors would like to gratefully acknowledge the Research Council of Norway and the partners of *Alpakka—Circular Aluminium Packaging in Norway* (NFR Project nr. 296276) for funding the project, Speira Holmestrand for the materials, and the Department of Materials Science and Engineering at NTNU, Trondheim, for the experimental equipment and support. On behalf of all authors, the corresponding author states that there is no conflict of interest.

Funding Open access funding provided by NTNU Norwegian University of Science and Technology (incl St. Olavs Hospital - Trondheim University Hospital).

References

1. Capuzzi S, Timelli SG (2018) Preparation and melting of scrap in aluminum recycling: a review. Metals 8(4):249. https://doi.org/10.3390/met8040249
2. van Schaik A, Reuter M (2014) Material-centric (aluminum and copper) and product-centric (cars, WEEE, TV, lamps, batteries, catalysts) recycling and DfR rules. In: Worrel E, Reuter M (eds) Handbook of recycling: state-of-the-art for practitiones, analyst and scientists. Elsevier, Amsterdam
3. Kvithyld A, Meskers C, Gaal S, Reuter M, Engh T (2008) Recycling light metals: optimal thermal de-coating. JOM 60:47–51. https://doi.org/10.1007/s11837-008-0107-y
4. Vallejo-Olivares A, Philipson H, Gökelma M, Roven HJ, Furu T, Kvithyld A, Tranell G (2021) Compaction of aluminium foil and its effect on oxidation and recycling yield. In: Perander L (ed) Light metals 2021. Springer, Cham
5. Rossel H (1990) Fundamental investigations about metal loss during remelting of extrusion and rolling fabrication scrap. In: Bickert CM (ed) Light metals 1990. Springer, Cham, pp 721–729
6. Peterson RD (1995) Issues in the melting and reclamation of aluminum scrap. JOM 47(2):27–29. https://doi.org/10.1007/BF03221402
7. Schmitz CJ (2014) Handbook of aluminium recycling: mechanical preparation, metallurgical processing, heat treatment. Vulkan-Verlag GmbH, Essen
8. Steglich J, Buchholz A, Aluminium H, Dittrich R, Friedrich B (2015) Conductive heat transfer in used beverage can scrap. In: Proceedings advances in materials & processing technologies, Madrid December 2015
9. Wells PA, Peterson RD (1990) Transient three-dimensional briquette preheater model. In: van Linden J, Stewart D, Sahai Y (eds) Proc. Second international symposium - reclying metals and engineered materials, Springer, Cham, pp 221–236
10. Steglich J, Friedrich B, Rosefort M (2020) Dross formation in aluminum melts during the charging of beverage can scrap bales with different densities using various thermal pretreatments. JOM 72:3383–3392. https://doi.org/10.1007/s11837-020-04268-4
11. Boin U, Reuter MA, Probst T (2004) Measuring - modelling: understanding the Al scrap melting processes inside a rotary furnace. World Metall ERZMETALL 57(5):266–271
12. Zhou B, Yang Y, Reuter MA, Boin UMJ (2006) Modelling of aluminium scrap melting in a rotary furnace. Miner Eng 19:299–308. https://doi.org/10.1016/j.mineng.2005.07.017
13. Capuzzi S, Timelli G, Capra L, Romano L (2019) Study of fluxing in Al refining process by rotary and crucible furnaces. Int J Sustain Eng 12(1):38–46. https://doi.org/10.1080/19397038.2017.1393022
14. Capuzzi S, Kvithyld A, Timelli G, Nordmark A, Gumbmann E, Engh TA (2018) Coalescence of clean, coated, and decoated aluminum for various salts, and salt-scrap ratios. J Sustain Metall 4:343–358. https://doi.org/10.1007/s40831-018-0176-2S
15. Thoraval DM, Friedrich B (2015) Metal entrapment in slag during the aluminium recycling process in tilting rotary furnace. In: Proceedings of EMC 2015, pp 359–367. https://doi.org/10.13140/RG.2.1.3436.8887
16. Xiao Y, Reuter MA, Boin U (2005) Aluminium recycling and environmental issues of salt slag treatment. J Environ Sci Heal 40(10):1861–1875. https://doi.org/10.1080/10934520500183824
17. Xiao Y, Reuter MA (2002) Recycling of distributed aluminium turning scrap. Miner Eng 15(11):963–970. https://doi.org/10.1016/S0892-6875(02)00137-1
18. Gökelma M, Diaz F, Öner IE, Friedrich B, Tranell G (2020) An assessment of recyclability of used aluminium coffee capsules. In: Tomsett A (ed) Light metals 2020. Springer, Cham
19. Wang M, Do Woo K, Kim DK, Ma L (2007) Study on de-coating used beverage cans with thick sulfuric acid for recycle. Energy Convers Manag 48(3):819–825. https://doi.org/10.1016/j.enconman.2006.09.008
20. Li N, Qiu K (2013) Study on delacquer used beverage cans by vacuum pyrolysis for recycle. Environ Sci Technol 47(20):11734–11738. https://doi.org/10.1021/es4022552
21. Önen R, Gökelma M (2022) Characteristics and behaviuor of coated aluminium scraps during thermal pre-treatment. In: Proceedings of ALUS 10th international aluminium symposium, pp 2016–210
22. Meskers C, Reuter M, Boin U, Kvithyld A (2008) A fundamental metric for metal recycling applied to coated magnesium. Metall Mater Trans B 39:500–517. https://doi.org/10.1007/s11663-008-9144-8
23. Meskers C, Xiao Y, Boom R, Boin U, Reuter M (2007) Evaluation of the recycling of coated magnesium using exergy analysis. Miner Eng 20(9):913–925. https://doi.org/10.1016/j.mineng.2007.02.006
24. Rombach G (2000) Verhalten mineralischer Pigmente beim Aluminiumrecycling. World Metall - Erzmetall 2(53):98–104
25. Hiraki T, Miki T, Nakajima K, Matsubae K, Nakamura S, Nagasaka T (2014) Thermodynamic analysis for the refining ability of salt flux for aluminum recycling. Materials (Basel) 7(8):5543–5553. https://doi.org/10.3390/ma7085543
26. Oosumi K (1994) Influence of paint on recycling of aluminum used beverage cans. In: Symposium K: environment conscious materials of the 3rd IUMRS international conference on advanced materials 1993, pp 197–200, https://doi.org/10.1016/B978-1-4832-8381-4.50051-2
27. Løvik NA, Müller DB (2014) A material flow model for impurity accumulation in beverage can recycling systems. In: Grandfield J (ed) Light metals 2014. Springer, Cham
28. Castro M, Remmerswaal J, Reuter M, Boin U (2004) A thermodynamic approach to the compatibility of materials combinations for recycling. Resour Conserv Recycl 43(1):1–19. https://doi.org/10.1016/j.resconrec.2004.04.011
29. Reuter MA, Van Schaik A, Gutzmer J, Bartie N, Abadías-Llamas A (2019) Challenges of the circular economy: a material, metallurgical, and product design perspective. Annu Rev Mater Res 49:253–274. https://doi.org/10.1146/annurev-matsci-070218-010057
30. Vallejo-Olivares A, Høgåsen S, Kvithyld A, Tranell G (2022) Effect of compaction and thermal de-coating pre-treatments on the recyclability of coated and uncoated aluminium. In: Eskin D (ed) Light metals 2022. Springer, Cham
31. Meskers CM (2008) Coated magnesium - designed for sustainability? PhD Thesis. ISBN: 978-9-064643-05-7
32. Steglich J, Dittrich R, Rombach G, Rosefort M, Friedrich B, Pichat A (2017) Dross formation mechanisms of thermally pretreated used beverage can scrap bales with different density, pp 1105–1113
33. Amini Mashhadi H, Moloodi A, Golestanipour M, Karimi EZV (2008) Recycling of aluminium alloy turning scrap via cold pressing and melting with salt flux. J Mater Process Technol

209(7):3138–3142. https://doi.org/10.1016/j.jmatprotec.2008.07.020